Biochimica et Biophysica Acta, 767 (1984) 209–216
Elsevier

BBA 41615

THE STATE OF MANGANESE IN THE PHOTOSYNTHETIC APPARATUS

3. LIGHT-INDUCED CHANGES IN X-RAY ABSORPTION (K-EDGE) ENERGIES OF MANGANESE IN PHOTOSYNTHETIC MEMBRANES *

DAVID B. GOODIN, VITTAL K. YACHANDRA, R. DAVID BRITT, KENNETH SAUER and MELVIN P. KLEIN

Laboratory of Chemical Biodynamics, Lawrence Berkeley Laboratory, University of California, Berkeley, CA 94720 (U.S.A.)

(Received April 3rd, 1984)
(Revised manuscript received July 2nd, 1984)

Key words: Oxygen evolution; ESR; Manganese; Photosystem II; X-ray absorption spectroscopy; (Spinach chloroplast)

Photosynthetic water oxidation by higher plants proceeds as though five intermediates, S_0–S_4, operate in a cyclic fashion. In this study of the manganese involvement in the process, a low temperature EPR signal is used as an indicator of S-state composition for manganese X-ray absorption K-edge measurements of a spinach Photosystem II preparation. A dramatic change is observed in the edge properties between samples prepared in states S_1 and either S_2 or S_3, establishing a direct relation between the local environment of Mn and the S-state composition. Samples in S_2 or S_3 exhibit a broadening of the principal absorption peak and a shift to higher energy by as much as 2.5 eV relative to S_1 samples. The magnitude of these changes is directly related to the EPR signal intensity induced by illumination. Models are discussed in which these data may be interpreted in terms of a conformation-induced change in Mn ligation and/or oxidation during the S_1 to S_2 transition.

Introduction

Kinetic studies of oxygen evolution by algae and higher plants have established the probable existence of five states, S_0–S_4, involved in the stabilization and storage of oxidizing equivalents generated at the Photosystem II (PS II) reaction center [1]. The identity of the S intermediates has not been established, but evidence implicates a form of membrane-bound manganese [2]. Broken, washed chloroplast preparations typically contain 4–6 Mn/PS II reaction center, and approx. 2/3 of this quantity is released by treatments such alkaline Tris washing, mild thermal shock or high salt incubation, that specifically inactivate O_2 evolution [3–5]. Recent work has shown that high salt washing [6] or treatment with alkaline Tris buffer releases proteins [7–9] that are associated with the functional stability of the oxygen-evolving complex. More recently, it has been reported that one of the peptides with a molecular weight of 32 kDa released by osmotic shock under oxidizing conditions contains two Mn atoms [10]. However, Ono and Inoue [11] report total solubilization of this protein without release of membrane Mn, a result that has been confirmed in our laboratory [40]. Although recent studies in this area with

* Parts 1 and 2 to this series are Refs. 30 and 25, respectively. Abbreviations: Chl, chlorophyll; DMBQ, 2,6-dimethyl-*p*-benzoquinone; Mes, 4-morpholineethanesulfonic acid; PS, photosystem; Tricine, *N*-[2-hydroxy-1,1-bis(hydroxymethyl)-ethyl]glycine.

0005-2728/84/$03.00 © 1984 Elsevier Science Publishers B.V.

inside-out thylakoids [12] and PS II particles [7] have given rise to a reevaluation of the Mn content per photosynthetic unit, it is clear that a direct relation exists between Mn and O_2 evolution.

More evidence for the direct involvement of manganese has been provided with the discovery of a light-induced EPR signal observed at low temperature in spinach chloroplasts [13]. This signal, containing 19 or more lines extending over more than 1000 G, was assigned to a manganese species on the basis of its hyperfine splittings. Simulation of the hyperfine structure is consistent with either a weakly exchange-coupled Mn(III, IV) binuclear or a Mn(III, III, III, IV) tetranuclear manganese center [14,15]. The temperature dependence of the light-induced formation and subsequent decay of this signal indicates that it is correlated with the presence of the S_2 state of the oxygen-evolving complex [16]. Studies on whole chloroplasts have shown that treatments that affect oxygen evolution, including alkaline Tris washing, cause the disappearance of this signal [15]. It was concluded that the signal arises from the oxygen-evolving complex, because restoration of PS II electron flow using artificial donors could be accomplished without the return of the signal.

We have used this EPR signal as an indicator of S-state composition and we report here a study of the X-ray absorption of Mn (K-edge) of a spinach PS II preparation stabilized in states S_1, S_2 or S_3.

Materials and Methods

Broken chloroplasts were prepared from destemmed market spinach by grinding in a Waring blendor for 10–15 s at 4°C in a buffer comprising 0.4 M NaCl/20 mM Tricine (pH 8.0)/2 mM $MgCl_2$/5 mM EDTA. The homogenate was strained through eight layers of cheesecloth and centrifuged at 4°C for 10 min at $6000 \times g$. The pellet was resuspended in 0.15 M NaCl/20 mM Tricine (pH 8.0)/5 mM $MgCl_2$ and spun at $500 \times g$ for 30 s. The supernatant was decanted through a Kimwipe and centrifuged at $6000 \times g$ for 10 min. The process of resuspension and pelleting was then repeated. Preparation of oxygen-evolving PS II sub-chloroplast membranes was accomplished by the method of Kuwabara and Murata [9].

Rates of oxygen evolution were measured using a Clark-type oxygen electrode biased at −0.6 V vs. Ag|AgCl. Illumination was with a 200 W quartz lamp filtered with Corning 3-68 and 1-56 glass filters. Samples were suspended at 20–30 μg Chl/ml in 20 mM Mes (pH 6.0)/20 mM NaCl/5 mM $MgCl_2$/500 μM DMBQ/1 mM $K_3Fe(CN)_6$/1 mM $K_4Fe(CN)_6$. Chlorophyll concentration was determined by the method of Arnon [17].

EPR measurements were performed on a Varian E-109 spectrometer equipped with a model E102 microwave bridge. Samples were run at 10–12 K in an Air Products liquid helium cryostat at a microwave frequency of 9.12 GHz using 100 kHz field modulation. Other instrument settings are provided in the figure legends. Measurements of the multi-line EPR signal were made by suspending samples at 2–5 mg Chl/ml in buffer containing 50% glycerol, which stabilises the membrane preparations when frozen and also facilitates the observation of the multiline EPR signal. Samples were incubated at 273 K for specified times in complete darkness before equilibration at 190 K in a Varian V 6040 NMR temperature controller and illumination with a 400 W tungsten lamp through a 5 cm water filter. After illumination, samples were immediately transferred to and stored at 77 K. All signal intensities were corrected for EPR tube volume.

X-ray absorption edge spectra were collected at the Stanford Synchrotron Radiation Laboratory, Stanford, CA on wiggler beam line VII-3 (unfocussed, $1 \cdot 10^{12}$ photons/s with 1 eV resolution) during dedicated operation of the SPEAR storage ring, providing 40–80 mA electron beams at 3.0 GeV using a Si⟨111⟩ double crystal monochromator. The ratios of the fluorescence, F, to incident intensity, I_0, were measured using an NE104 plastic scintillation array similar to that described by Powers et al. [18], equipped with Cr fluorescence filters and Soller slit assembly [19]. The filter consisted of 0.25 mm thick Be with Cr electro-deposited to a thickness of 0.013 mm. Energy calibration was maintained by simultaneous measurement of the 'white line' pre-edge feature of $KMnO_4$ at 6543.3 eV [20].

X-ray absorption samples were prepared by layering pellets of spinach PS II membranes in 50% glycerol/50 mM Mes (pH 6.0)/15 mM

NaCl/5 mM $MgCl_2$ at approx. 8 mg Chl/ml (100–200 μM Mn) into narrow lucite sample cells with an open cavity of dimensions $5 \times 30 \times 2$ mm. Dark adaptation, illumination and EPR measurements were carried out directly in these sample cells. The exact incubation and illumination protocols are described with the results. During X-ray measurements, samples were suspended in a jacketted N_2 boil-off jet maintained at 170–190 K in darkness. After pre-edge background subtraction, the X-ray edge inflection point energy was determined by fitting quadratic polynomials over fixed 8 eV energy regions evenly spaced about each point in the spectrum. This 8 eV energy region was chosen because it is just large enough to smooth the statistical noise in the first derivative spectrum. The derivative of the fitted polynomial was taken as an approximation to the true first derivative at that point.

Results

X-ray absorption experiments

We have measured the Mn X-ray absorption K-edge of spinach PS II preparations for dark-adapted and for illuminated samples exhibiting the multi-line EPR signal. The samples used had high rates of oxygen evolution (526 μmol O_2/mg Chl per h) at pH 6.3 with DMBQ as acceptor) and a Mn/Chl mole ratio of 0.0143. This corresponds to 3.6 Mn per reaction center assuming a photosynthetic unit of 250 Chl [21]. Sample A was prepared in state S_1 by illumination for 60 s at 190 K followed by dark adaptation for 1 h at 273 K. This preillumination was given to reduce the S_0 concentration, which would otherwise constitute about 25% of the oxygen-evolving complex centers. Samples B and C were prepared in state S_2 by first generating S_1 according to the above procedure followed by 60 s illumination at 190 K. For sample D, an attempt to generate S_3 was made in which S_2 was prepared as above, followed by warming the sample in the dark for 5–10 s to 273 K. This procedure was followed by illumination for 60 s at 190 K. All samples were immediately transferred to and stored at 77 K.

The S_3 protocol was based on the knowledge that only one equivalent of electrons is transferred at 190 K because reoxidation of Q^- is blocked [22]. Any additional excitation reaching the reaction center will then result in rapid charge recombination between $P680^+$ and I^-. At 273 K, the reoxidation of Q^- is much faster than S_2 relaxation [16], so that brief warming to this temperature prepares the reaction center for another one-equivalent transfer.

Low temperature (10 K) EPR spectra were recorded for samples A–D prior to the X-ray absorption measurements. The results (Fig. 1) indicate the absence of the multi-line signal in the S_1 sample, its presence in the two S_2 samples and a significant reduction of the amplitude for the S_3 sample. The amplitudes of the EPR signals measured before and after X-ray data collection are presented in Table I. Only sample B showed a significant change in EPR signal amplitude afterwards. We attribute this reduction in EPR signal amplitude to the relaxation of S_2 to S_1 either during transfer of samples to and from the liquid N_2 dewar to the X-ray sample holder or during X-ray data collection. We discount any significant radiation damage as a cause for this decay, because the oxygen-evolution activity of the samples before and after X-irradiation was not significantly different from control samples. No effect

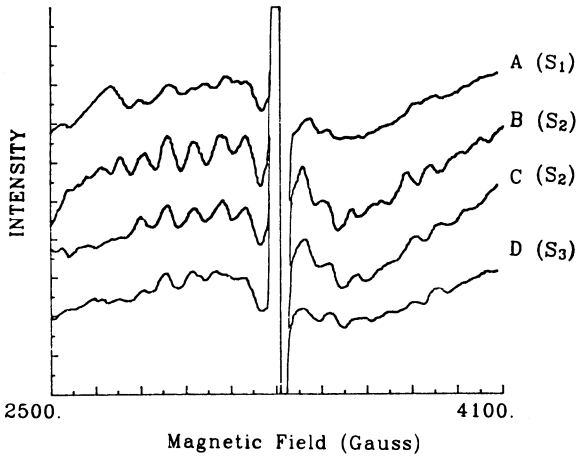

Fig. 1. Multi-line EPR spectra observed for spinach PS II sub-chloroplast samples used for X-ray absorption edge studies. EPR spectra were recorded at 14 K using 100 mW microwave power at 9.22 GHz, 100 KHz field modulation of 32 G, scan time 4 min and time-constant 0.25 s. Illumination protocols for the various S states are described in the text. The samples are: A, S_1; B, S_2; C, a second S_2; D, S_3.

TABLE I

MULTI-LINE EPR AMPLITUDE FOR X-RAY EDGE SAMPLES OF SPINACH PS II MEMBRANES

EPR amplitudes before and after X-ray absorption edge spectroscopy (XAES) were calibrated with an S_2 sample that was not exposed to the X-ray beam. The signal amplitudes were taken as the average peak-to-peak height of four lines downfield from $g = 2$

Sample	Multi-line amplitude (arbitrary units)	
	before XAES	after XAES
A (S_2)	1.5	1.7
B (S_2)	5.5	2.9
C (second S_2)	4.0	*
D (S_3)	2.0	2.3

* This sample was used to prepare a S_1 sample by allowing it to relax in the dark over ice for 1 h (sample E).

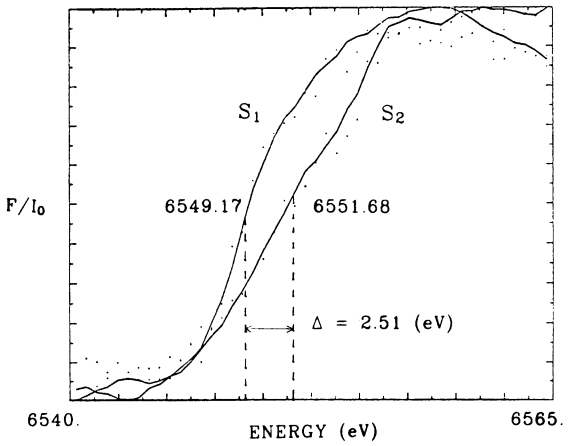

Fig. 3. X-ray absorption edge spectra of Mn in spinach PS II preparations in the S_1 or S_2 states, on an expanded energy scale.

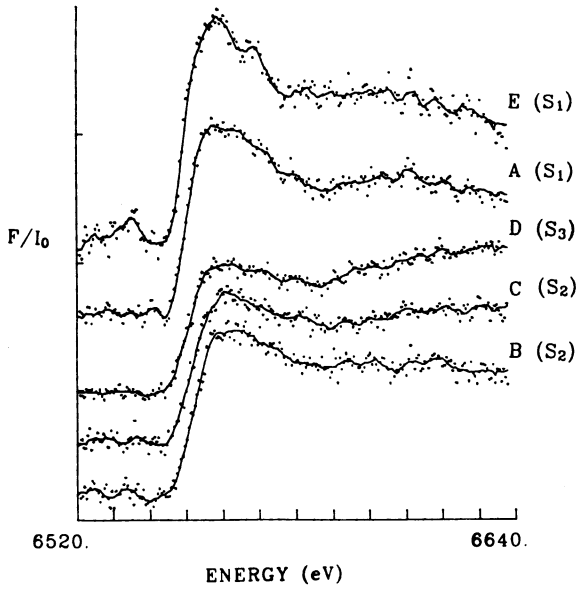

Fig. 2. X-ray absorption edge spectra of Mn in spinach PS II preparations. Data were collected for samples at 170–190 K as described in Materials and Methods. Each edge is the sum of 20–30 individual 20-min scans. A background has been removed, which sets the absorption at energies lower than the edge to zero. Data were collected by fluorescence, F, and I_0 is the incident intensity. The samples are: A, S_1; B, S_2; C, a second S_2; D, S_3; and E, S_1 prepared from sample C, after its edge was recorded, by dark adaption for 1 h at 273 K in total darkness. The low-energy features in sample E that are missing in the other samples are due to differences in S/N and are not inherent differences in the spectra.

on the EPR signal amplitude after repeated cycling between the storage temperature of 77 K and the X-ray measurement temperature of 175 K was observed for control samples.

The Mn X-ray K-edge spectra for these samples are presented in Fig. 2. The S_2 sample (B) shows a significantly broader principal absorption maximum and, possibly as a result, a shift to higher energy relative to the S_1 sample (A). The shift in energy is seen more clearly in Fig. 3 which shows the superimposed Mn K-edge spectra of samples E (S_1) and B (S_2) on an expanded scale. The second S_2 sample (C) edge is consistent with the first (B); further, a 1-h dark adaptation of this sample

TABLE II

K-EDGE INFLECTION POINT ENERGIES FOR SPINACH PS II SAMPLES

Derivatives were obtained from a 25-point sliding fit to a second-order polynomial (8 eV per fit). avg., average.

Sample	K-edge inflection (eV)	
A (S_1)	6549.9	avg. S_1 = 6549.6
E (S_2 relaxed to S_1)	6549.2	
B (S_2)	6551.7	avg. S_2 = 6551.3
C (second S_2)	6550.9	
D (S_3)	6550.2	

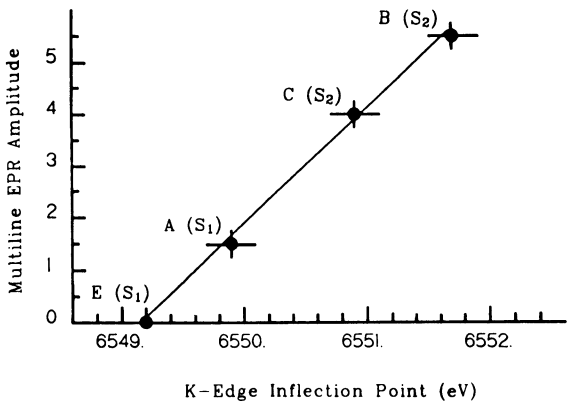

Fig. 4. A plot of the amplitudes of the multi-line EPR signal for illuminated spinach PS II membrane samples versus the K-edge inflection point energies; from data shown in Figs. 1 and 2.

(labeled E) over ice, a procedure known to relax S_2 to S_1, also regenerates the edge observed for S_1. The K-edge for S_3 (D) is quite similar to those observed for S_2. The small difference in shape between S_2 and S_3 that is observed may not be meaningful, because differences of a similar magnitude are also observed for the two S_2 samples.

The edge inflection point energies for these spectra are presented in Table II. The energies differ from one another by much more than the estimated uncertainty of ± 0.2 eV for any one sample, thus indicating the presence of a slightly different S-state composition for each sample. Fig. 4 shows that the edge inflection points for S_1 and S_2 samples are in fact well-correlated with the observed multi-line EPR signal intensities.

The lowest edge inflection energy is observed for the freshly dark-adapted S_1 sample, while the highest inflection energy is from one of the S_2 samples. The energy difference between these samples, illustrated in Fig. 3, is 2.51 eV. The average edge shift observed between the S_1 and S_2 samples is 1.78 eV.

Discussion

A large reproducible change is observed in the manganese K-edge X-ray absorption spectra of PS II samples prepared in states S_1 or S_2. Changes of the nature observed are classic behavior for loss of ligand symmetry caused by metal oxidation and/or forced ligand geometry distortion [23]. For example, in ionic compounds such as ferrous and ferric fluorides, oxidation causes an increase to higher energy of about 5 eV in the iron absorption edge [24]. For covalent compounds such as ferro- and ferricyanides, the increase is much smaller, the edge energy being roughly 1 eV higher for the oxidized iron salt. Changes in the shape of the edge between the oxidized and the reduced forms are not appreciable, because the geometries of both forms are about the same. Broadening of the edge is often observed and attributed to the splitting of the $1s$–$4p$ transition into as many as three features, owing to lowering of symmetry. In a purely cubic case, the splitting reduces to zero, while the maximal splitting is observed for square planar geometry. Broadening of the edge may also be due to an increase in the intensity of the $1s$–$4s$ transition, an indication of a departure from axial symmetry [24].

It is probable in our samples that only a portion of the total pool of manganese contained in the photosynthetic membranes is contributing to the observed change. The effect of a shift of the absorption of one pool with respect to that of the other is to broaden the principal absorption maximum in a manner similar to that observed.

From previous correlations of manganese edge inflection point energies [25], we expect an edge shift of approx. 2.3 eV per unit change in coordination charge, which is the formal oxidation state corrected for covalency [26]. Some typical changes observed in metallo-proteins for unit change in oxidation state per metal atom are about 3 eV for the Cu edge in Cu-Zn superoxide dismutase [27], 3–4 eV for the Cu edge in plastocyanin and cytochrome oxidase [28], 2 eV for the Fe edge in cytochrome *c* and cytochrome oxidase [24,28] and about 1.5 eV change for the Mn edge in Mn superoxide dismutase (Goodin et al., unpublished data). The simplest interpretation of the multi-line EPR signal associated with S_2 is that only one charge equivalent per P-680 has been transferred. The observed S_1 to S_2 average K-edge shift of 1.78 eV is larger than one would expect if only one electron equivalent is removed from a total pool of 3.6 manganese atoms.

There is a number of explanations possible for this observation. The first is that the photosyn-

thetic unit size of the preparation is much smaller than that reported [21,29], which would result in fewer manganese per PS II than assumed. Alternatively, one pool of manganese may be involved in a structural role while another has a functional role. One-electron oxidation of the functional manganese center during the S_1 to S_2 transition may cause a change in the conformation of neighboring proteins, altering the environment of the structural manganese and causing a change in the Mn K-edge energy. However, a large conformational change is not expected to occur at the illumination temperature. Finally, it is possible that more than one charge equivalent is transferred from the Mn in the oxygen-evolving complex under the illumination conditions used. This would occur if, for example, one oxidizing equivalent is stored on a PS II electron carrier other than manganese in S_1. Transition to state S_2 would then cause the removal of both reducing equivalents from the manganese center.

In regard to proposed oxidation states of manganese sites in these centers, the combination of the X-ray edge data with the fact that the S_2 state contains a paramagnetic species is of great utility. The edge positions of PS II samples in state S_1 (6549.6 eV) are similar to and slightly higher in energy was observed in a previous study on dark-adapted whole chloroplasts (6549.1 eV) [25]. In that study, we reported the Mn K-edge positions of Mn(II)(aqueous) at 6548.5 eV, $Mn(III)(acac)_3$ at 6550.7 eV and Mn(IV, IV) di-μ-oxo dimeric complex (di-μ-oxotetrakis(1,10-phenanthroline)dimanganese perchlorate) at 6551.0 eV. Based on these results, we proposed that the average manganese oxidation state in dark-adapted membranes lies between II and III. For the dark-adapted PS II preparation, which contains a lower and presumably more homogeneous manganese content than do chloroplasts, the edge position also lies between those of observed Mn(II) and Mn(III) complexes. The average inflection position observed for samples prepared in S_2 by low temperature illumination (6551.3 eV) is very similar to that observed for the Mn(IV, IV)) di-μ-oxo dimeric compound and strongly suggests a Mn(IV) oxidation level. The oxidation state of Mn in state S_3 is more uncertain, because its edge inflection point is between that of S_1 and S_2. But the shape of the edge is significantly different from S_1 and closely resembles that of S_2. We speculate that the oxidation state of S_3 is similar to that of S_2, but that S_3 is structurally distinct from either S_1 or S_2.

There is evidence that the oxygen-evolving complex consists of exchange-coupled metal centers [14], and a number of models for the site have included dimeric manganese species [2,30,31]. Based on the observation that state S_2 is paramagnetic, Dismukes et al. [14] have proposed that it contains a Mn(III, IV) complex; the edge properties observed in this work are consistent with that assignment. If it is true that two oxidizing equivalents are added to the manganese center accompanying the S_1 to S_2 transition, as discussed above, these observations would be consistent with the presence of a Mn(II, III) complex in S_1 and Mn(III, IV) in S_2. However, a Mn(III, III) complex which undergoes a large change in ligation in the S_1 to S_2 transition could also give rise to the observed properties.

It is possible to incorporate the S state oxidation levels indicated in the present work into a speculative but consistent model of the oxygen-evolving complex that is similar in nature to the ones described earlier [31,32]. In the present scheme (Scheme I), the oxygen-evolving complex contains two closely coupled manganese centers and two species labeled D, possibly serving as ligands to the metal, which are themselves capable of electron donation. It would still be consistent with Scheme I if the species labelled D_1 and D_2 were a single chemical moiety but capable of two electron transfer. Extraction studies have implicated quinones as components on the donor side of Photosystem II [33]. Multimeric manganese semiquinone complexes have been reported, and some of these complexes indeed exhibit two-electron metal-ligand transfer equilibria similar to that suggested in the model [34]. In addition, our model includes deprotonation steps to explain the proton release pattern of 1, 0, 1, 2 [35], although it is as yet inconclusive, because other work [36] indicates that the pattern is 0, 1, 1, 2.

One of the unique features of this model is that charge is transferred onto the metal centers only after the ligated donor species (D) have been oxidized by one equivalent each. This mode of transfer, in which oxidation of a ligand occurs

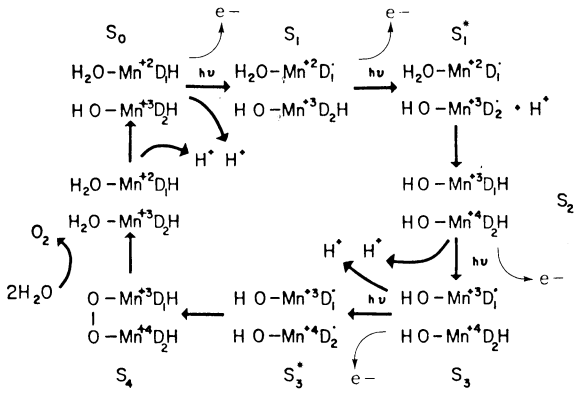

Scheme I. A proposed scheme for the change in manganese oxidation associated with S-state cycling. In state S_0, the metal centers are in the Mn(II,III) state. Transition from S_0 to S_1 occurs by the oxidation of one of the donor species (DH), with the release of a proton. The following transition occurs first by oxidation of the second donor (DH) species to give the hypothesized unstable intermediate S_1^*. This state relaxes to S_2 after two charge equivalents are transferred from the donor species to Mn, giving the Mn(III,IV) complex, with no net proton release. Transition from S_2 to S_3 is analogous to the S_0 to S_1 step. The final light-induced step proceeds as before with the formation of an unstable intermediate S_3^*, which relaxes to S_4, a peroxo bridged species, with the Mn(III,IV) species containing the reduced donors (DH). A water-ligand exchange reaction may then accompany the release of O_2, regenerating S_0. The last step proposes the release of two protons, one before and one after release of O_2.

prior to the transfer of charge onto the metal species, provides a convenient means by which oxidizing equivalents may be moved from the outer to the inner coordination sphere of the metal. In contrast to the behavior of many electron-transfer proteins, in which the metal is directly oxidized or reduced, this kind of process is thought to be kinetically slower and may result in longer lived oxidized intermediates, because a change in oxidation level necessarily involves a perturbation or rearrangement of the ligand species. These arguments have been used in favor of this type of mechanism for electron-storage as opposed to simple one-electron-transfer enzymes [14].

As in the model proposed by Renger [31], our scheme involves a significant smearing out of charge from the manganese center onto ligands, avoiding the use of highly oxidized manganese species. In fact, the scheme employs only two formal oxidation levels for the manganese center: Mn(II, III) and Mn(III, IV). However, unlike the additional donor proposed by Renger, the oxidized forms of DH are not held throughout the S state cycle, but are instead proposed to play an intimate role in the redox reactions. Scheme I is fairly consistent with that proposed by Wydrzynski, Sauer and Govindjee et al. [32,37] in that S_1 contains a Mn(II, III) species, and S_3 contains manganese with an oxidation level that is similar to that in S_2, which we suggest is Mn(III, IV).

Other than accounting for the large change in manganese oxidation level between S_1 and S_2 indicated by the present work, the scheme has several attractive features. It is indicated from the model that the oxidation level of the manganese site may not be significantly altered in the transition from S_2 to S_3, where oxidation of D_1H is instead possible. Behavioral similarity of S_2 and S_3 is often observed. For example, both states appear to be the sites of Tris or NH_3 inactivation [38,39]. An explanation for the dark relaxation of S_2 and S_3 may also be inherent in such a model, because they are the only metastable states containing manganese in the higher oxidation states. The EPR relaxation properties of S_2 and S_3 may be determined by the differences in the interaction of the Mn spin system with DH and D$^{\cdot}$, respectively. Such an interaction is entirely consistent with the observation that our attempt to generate S_3 caused most of the multi-line EPR signal to disappear, but the sample shows an absorption edge that is not very different from that of the S_2 samples. This brings up the question of whether the Mn(II, III) complex in state S_1 might be expected to exhibit EPR signals. The additional spin on the ligand D should alter the relaxation properties of such a signal in a manner analogous to that proposed for the state S_3. If the spins were strongly coupled, an integral spin state should result, exhibiting greatly altered or no EPR properties et all. A broad multi-line EPR signal attributed to manganese in state S_1 that could be observed only at temperatures below 8 K at high power levels was reported recently [10]. Such behavior suggests an efficient relaxation mechanism.

Conclusion

The experiments reported here demonstrate conclusively that manganese atoms participate in

the light-driven electron-transfer reaction associated with water oxidation at Photosystem II and are themselves oxidized as the oxygen-evolving complex advances from the S_1 to S_2 state.

Acknowledgements

We thank Ann McDermott, Sun Un and Ron Guiles for help with the data collection. Dr. John Dini of the Lawrence Livermore National Laboratory kindly fabricated the electrodeposited Be filters. This work was supported by the Office of Energy Research, Office of Basic Energy Sciences, Biological Energy Research Division of the U.S. Department of Energy under Contract No. DE-AC03-76SF00098, and NSF Grant PCM82-16127. Synchrotron radiation facilities were provided by the Stanford Synchroton Radiation Laboratory which is supported by the U.S Department of Energy, Office of Basic Energy Sciences, and by the National Institutes of Health, Biotechnology Resource Program, Division of Research Resources.

References

1 Forbush, B., Kok, B. and McGloin, N.P. (1971) Photochem. Photobiol. 14, 307–321
2 Sauer, K. (1980) Acc. Chem. Res. 13, 249–256
3 Cheniae, G.M. and Martin, I.F. (1970) Biochim. Biophys. Acta 197, 219–239
4 Blankenship, R.E. and Sauer, K. (1974) Biochim. Biophys. Acta 357, 252–266
5 Blankenship, R.E., Babcock, G.T. and Sauer, K. (1975) Biochim. Biophys. Acta 387, 165–175
6 Åkerlund, H.-E., Jansson, C. and Andersson, B. (1982) Biochim. Biophys. Acta 681, 1–10
7 Henry, L.E.A., Lindberg Møller, B., Andersson, B. and Åkerlund, H.-E. (1982) Carlsberg Res. Commun. 47, 187–198
8 Yamamoto, Y., Doi, M., Tamura, N. and Nishimura, M. (1981) FEBS Lett. 133, 265–268
9 Kuwabara, T. and Murata, N. (1982) Plant Cell Physiol. 23, 533–539
10 Dismukes, G.C., Abramowicz, D.A., Ferris, K.F., Mathur, P., Siderer, Y., Upadrashta, B. and Watnick, P. (1983) in The Oxygen Evolving System of Photosynthesis, (Inoue, Y. et al., eds.), pp. 145–148, Academic Press, Tokyo
11 Ono, T.-A. and Inoue, Y. (1983) FEBS Lett. 164, 255–260
12 Mansfield, R. and Barber, J. (1982) FEBS Lett. 140, 165–168
13 Dismukes, G.C. and Siderer, Y. (1981) Proc. Natl. Acad. Sci. USA 78, 274–278
14 Dismukes, G.C., Ferris, K. and Watnick, P. (1982) Photobiochem. Photobiophys. 3, 243–256
15 Hansson, Ö. and Andréasson, L.-E. (1982) Biochim. Biophys. Acta 679, 261–268
16 Brudvig, G.W., Casey, J.L. and Sauer, K. (1983) Biochim. Biophys. Acta 723, 366–371
17 Arnon, D.I. (1949) Plant Physiol. 24, 1–15
18 Powers, L., Chance, B., Ching, Y. and Angiolillo, P. (1981) Biophys. J. 34, 465–498
19 Stern, E.A. and Heald, S.M. (1979) Rev. Sci. Instrum. 50, 1579–1582
20 Goodin, D.B., Falk, K.-E., Wydrzynski, T. and Klein, M.P. (1979) 6th Annual Stanford Synchrotron Radiation Laboratory Users Group Meeting, SSRL Report No. 79/05, 10–11.
21 Babcock, G.T., Ghanotakis, D.F., Ke, B. and Diner, B.A. (1983) Biochim. Biophys. Acta 723, 276–286
22 Joliot, A. (1974) Biochim. Biophys. Acta 357, 439–448
23 Srivastava, U.C. and Nigam, H.L. (1972) Coord. Chem. Rev. 9, 275–310
24 Shulman, R.G., Yafet, Y., Eisenberger, P. and Blumberg, W.E. (1976) Proc. Natl. Acad. Sci. USA 73 (5), 1384–1388
25 Kirby, J.A., Goodin, D.B. Wydrzynski, T., Robertson, A.S. and Klein, M.P. (1981) J. Am. Chem. Soc. 103, 5537–5542
26 Ovsyannikova, I.A., Batsanov, S.S., Nasonova, L.I., Batsanova, L.R. and Nekrasova, E.A. (1967) Bull. Acad. Sci. USSR., Phys. Ser. (Engl. Transl.) 31, 936
27 Blumberg, W.E., Peisach, J., Eisenberger, P. and Fee, J. (1978) Biochemistry 17, 1842–1846
28 Hu, V.W., Chan, S.I. and Brown, G.S. (1977) Proc. Natl. Acad. Sci. USA 74, 3821–3825
29 Lam, E., Baltimore, B., Ortiz, W., Chollar, S., Melis, A. and Malkin, R. (1983) Biochim. Biophys. Acta 724, 201–211
30 Kirby, J.A., Robertson, A.S., Smith, J.P., Thompson, A.C., Cooper, S.R. Klein, M.P. (1981) J. Am. Chem. Soc. 103, 5529–5537
31 Renger, G. (1978) in Photosynthetic Oxygen Evolution (Metzner, H., ed.), pp. 229–248, Academic Press, London
32 Wydrzynski, T. and Sauer, K. (1980) Biochim. Biophys. Acta 589, 56–70
33 Kohl, D.H. and Wood, P.M. (1969) Plant Physiol. 44, 1439–1445
34 Lynch, M.W., Valentine, M. and Hendrickson, D.N. (1982) J. Am. Chem. Soc. 104, 6982–6989
35 Fowler, C.F. (1977) Biochim. Biophys. Acta 462, 414–421
36 Junge, W., Renger, G. and Ausländer, W. (1977) FEBS Lett. 79, 155–159
37 Govindjee, Wydrzynski, T. and Marks, S.B. (1977) in Bioenergetics of Membranes (Packer, L., Papageorgiou, G.C. and Trebst, A., eds.), pp. 305–316, Elsevier, New York
38 Cheniae, G.M. and Martin, I.F. (1978) Biochim. Biophys. Acta 502, 321–344
39 Velthuys, B.R. (1975) Biochim. Biophys. Acta 396, 392–401
40 Blough, N.V. and Sauer, K. (1984) Biochim. Biophys. Acta 767, 376–380